Refereed Proceedings

The 12th International Conference on Fluidization - New Horizons in Fluidization Engineering

Engineering Conferences International   *Year* 2007

Dynamic Response Characteristics of Local Capacitive Measurement Devices with Application to CFD Validation

Clay R. Sutton*   John Chen†

*ExxonMobil Research & Development Company, clay.r.sutton@exxonmobil.com
†Lehigh University, jcc0@lehigh.edu

DYNAMIC RESPONSE CHARACTERISTICS OF LOCAL CAPACITIVE MEASUREMENT DEVICES WITH APPLICATION TO CFD VALIDATION

Clay R. Sutton* and John C. Chen†
*ExxonMobil Research & Engineering Company, Fairfax, VA 22311, USA
† Dept. of Chemical Engineering, Lehigh University, Bethlehem, PA 18015, USA

ABSTRACT

The Two-Fluid Model (TFM) approach to modeling fluid-solid systems holds great promise as a means to simulate arbitrary systems, thus greatly reducing design and scale-up efforts. Unfortunately, comprehensive experimental validations of these models are still in short supply. This work addresses this issue by proposing a framework under which to relate computational fluid dynamics model results with experimental measurements on a one-to-one basis. Specifically this is performed for the case of local solids concentration transients in a bench-scale bubbling fluidized bed. The manner in which this comparison is performed has implications for the conclusions that may be drawn for a given validation effort.

INTRODUCTION

Recently there has been an increased call for careful validation of CFD models (1). Particularly, these models should be validated on the basis of their ability to predict dynamic behavior (i.e., 2,3). Dynamic measurements are often difficult, and efforts must be made to ensure that the measurement technique doesn't induce any error that may alter conclusions about the extent of validation. For instance, this has been addressed in the literature for pressure transducer measurements (4). In a previous study, the TFM was challenged experimentally on a local transient basis (2). This approach was selected because time-averaged measurements are not necessarily sensitive to the nature of the heterogeneous structure present (e.g., bubbles, clusters). Due to the large contribution of these structures to solids mixing – and therefore transport and kinetics – it is absolutely critical to ensure that the model adequately captures them. This work employs a capacitive measurement technique, which despite having excellent frequency response characteristics, has a nonlinear sampling volume of a finite size.

Needle-type capacitance probes were utilized to measure the local instantaneous solids holdup in a bench-scale bubbling fluidized bed. The MFIX code (5) was employed for CFD calculations. Because of the finite sampling volume associated with this measurement technique, for comparison purposes it is not generally appropriate to study the fluctuations in a single computational node. In order to resolve features such as bubble clouds and void streamers in a bubble wake, it is

The 12th International Conference on Fluidization - New Horizons in Fluidization Engineering, Art. 87 [2007]

necessary to adopt a grid size smaller than the experimental sampling volume, and therefore multiple computational cells are required to draw accurate comparisons between experimental measurements and the CFD solution. Moreover, it is recognized that for electrostatic-based measurement instruments, the electric field attenuates with increasing distance from the measurement device, and that the relative contribution of a point to the measured holdup should be in direct proportion to the field strength at that point.

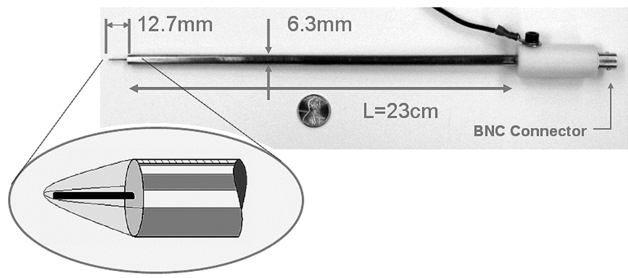

The normalized electric field strength in the vicinity of the capacitance probe was computed by numerical solution of the Poisson equation. This solution was used in turn to compute a matrix of weighting coefficients, which were applied to CFD model results. It is shown that computational cells on the order of 10^{-2}m away from the probe may contribute to the measured holdup. Therefore it is important to quantify this effect when considering results of statistical, spectral, and dynamical analyses. This is especially true when one wishes to draw comparisons between simulation and experiment.

THEORY

Capacitance Probe Field

Solids concentration time series are measured via needle-type capacitance probes. The probes were developed in-house at the Institute for Thermo-Fluids at Lehigh University (Fig 1). Further details of the probe construction and electronics are reported elsewhere (e.g., 6). The probes have a diameter of 6.3mm with an electrode tip length of 12.7mm. The central electrode diameter is 0.8mm in diameter. In order to roughly approximate the electric field in the vicinity of the needle-type capacitance probe tip, a stationary field is assumed. In classical electrostatics, the steady-state potential field is described by the following equations:

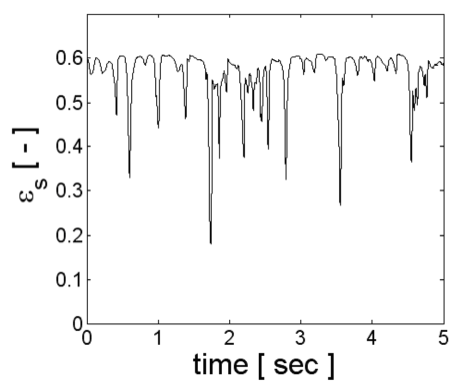

Figure 2. Typical solids concentration time-series.

$$\nabla \cdot \left(\varepsilon_0 \nabla V\right) = \rho$$
$$\mathbf{E} = \nabla V \qquad \text{(1a,b)}$$

As a first step, we consider the field in the absence of any charged particles. In a vacuum the charge density is zero, and therefore the potential field may be calculated by solving Laplace's equation with appropriate boundary conditions:

$$\nabla^2 V = 0 \tag{2}$$

Neglecting the azimuthal direction, Laplace's equation in cylindrical coordinates is given as:

$$\nabla^2 V = \frac{1}{r}\frac{\partial}{\partial r}\left(r\frac{\partial V}{\partial r}\right) + \frac{\partial^2 V}{\partial z^2} = 0 \tag{3}$$

The magnitude of the electric field may then be determined by finding the Euclidian norm of the vectors obtained by taking the gradient of the scalar potential field (as in equation 1). Dirichlet boundary conditions were applied the surfaces corresponding to the active guard tube and the central electrode. Both potentials were set to the RMS voltage for the capacitance bridge -8.5Vrms. We exploit axisymmetry about the θ and z axes, and surround this by a solution domain extending a sufficient distance from the probe. The surface of the solution domain was set to a constant zero potential, except where it was coincident with the z-axis of the probe. Here a Neumann boundary condition was applied reflecting the natural symmetry here (i.e., dV/dr = 0). The magnitude of the electric field was then calculated by equation (1b). This is plotted in Figure 3, which clearly indicates strong non-linearities within the sampling volume. Another important feature evident from this analysis is that the measurement volume retaining a significant strength extents well beyond the dimensions of the physical probe.

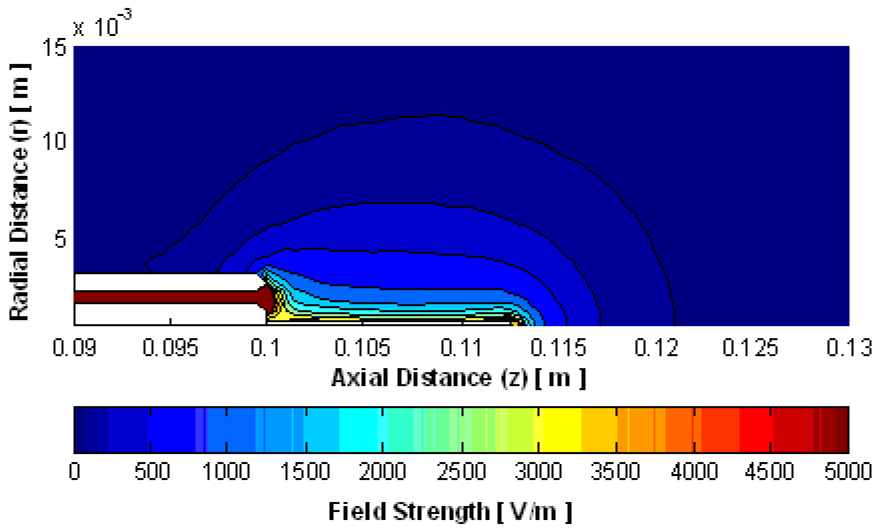

Figure 3. Numerical solution of electric field strength in vicinity of capacitance probe.

While this analysis could be extended to three dimensions, the CFD work here could only be performed in two, thus arises the need to average the resulting electric field strength in the axial direction in the vicinity of the tip (neglecting of course those points which fall within the body of the probe, itself). This is depicted in Figure 4. The resulting points are fit to a function of the form:

$$\mathbf{E}(r) = \alpha\frac{1}{r^{\beta}} \tag{4}$$

The decay exponent, β was determined to be 1.5. At a radial distance of 2.5cm from the probe centerline the field has diminished to about 2% of its maximum strength. This result is significant in that the measurement volume is of the same order of magnitude as the fluidization bubbles for a mildly fluidized system. For a CFD simulation using computational cells on the order of 0.33x0.33cm (as was done for the present work) this would translate to a region of 15x15 cells.

Constructing an Averaging Kernel

Based on the above information, a matrix of weighting coefficients was constructed in order to perform spatial averaging on simulated solids concentration fluctuations. By revolving the function calculated in equation 4 about $r = 0$, a surface is generated. Interpolated values of points on this surface corresponding to the centers of computation nodes in the simulation are tabulated in a matrix and normalized. This matrix (pictured graphically in Fig 4) then represents a normalized averaging kernel W that may be convolved with appropriate CFD cells. For an arbitrary point in the computational domain located a sufficient distance from the boundary, the averaged solids concentration signal is computed by:

$$\varepsilon_s(m,n) = \sum_{\mu}\sum_{\nu}\varepsilon_s\left(m+\mu-\frac{M+1}{2}, n+\nu-\frac{N+1}{2}\right)W(\mu,\nu) \qquad (5)$$

where M and N represent the lengths of the averaging kernel.

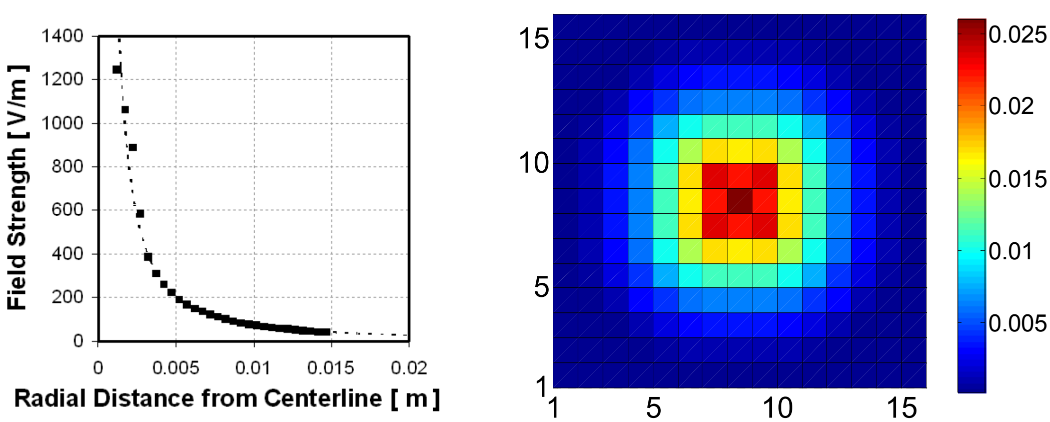

Figure 4. Radial profile of axially averaged field strength with line of best fit (left); visual representation of the normalized weighting matrix (right).

EXPERIMENT AND SIMULATION

In order to test the utility of this approach, a simple test case was devised to compare CFD results with experimental data. The experimental setup has been described in detail (e.g., 6) elsewhere. It is essentially a small bubbling fluidized bed (cross-section 14x23cm) with a porous plate distributor. 275μm glass beads (ρ_g = 2.6g/cm^3) were chosen as the fluidization media with a settled bed height of 30cm. The beads were fluidized at a superficial gas velocity of 12.17cm/s. A needle-type capacitance probe 6.3mm in diameter was inserted into the center of the bed 2.54

and 17.15cm above the distributor. Time series were logged at 300Hz for a time period of 60sec.

CFD simulations were carried out in 2-dimensions in order to generate solids concentration for comparison. For these purposes the MFIX code was utilized. Specific details regarding the simulation parameters are described in Sutton and Chen (2). With the exception of the particle diameter and superficial gas velocity the simulation parameters are identical to the previous work. The simulations were run for a time period of 30 seconds after the initial transient behavior was broken.

RESULTS AND DISCUSSION

Table 1 illustrates the impact of averaging on the predicted mean, standard deviation and average cycle frequency. Experimental time-series invariants measured at two elevations are compared side-by-side with those extracted from the CFD simulation from a single CFD cell, and finally with those computed using the averaging kernel. The first row considers the mean solids concentration; the mean is insensitive to the extent of averaging performed. In the second row we examine the standard deviation of the signals. Here the magnitude decreases a significant amount upon averaging. The application of the averaging kernel also brings the model prediction closer in line

Table 1. Comparison of CFD validation parameters with experiment.

	Z, cm	Experiment	Single CFD Cell	Averaged CFD Cells
Mean	2.54	*0.54*	*0.53*	*0.53*
	17.15	*0.57*	*0.53*	*0.53*
Std Dev	2.54	*0.011*	*0.09*	*0.025*
	17.15	*0.058*	*0.14*	*0.063*
ACF, Hz	2.54	*1.53*	*5.83*	*3.27*
	17.15	*1.87*	*5.65*	*3.18*

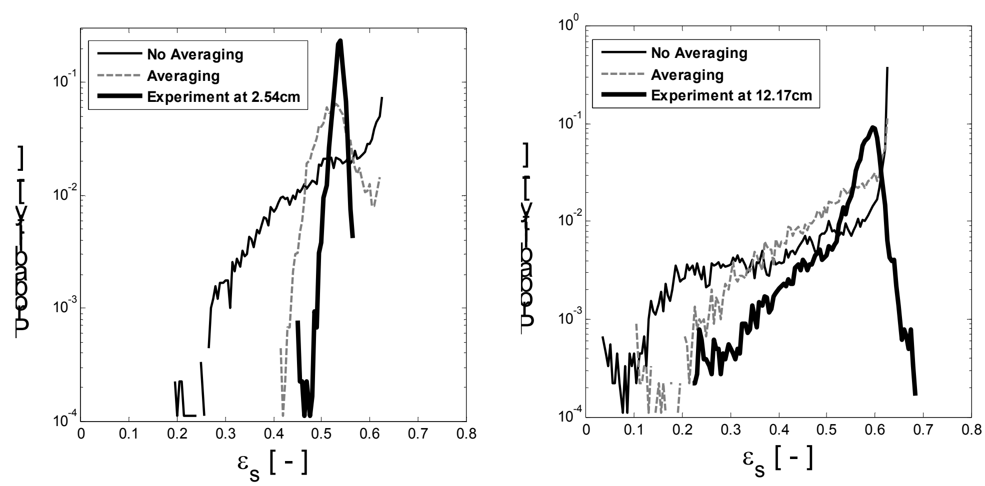

Figure 5. Solids concentration probability distributions measured 2.54cm above the distributor (left) and 17.15cm above the distributor (right). Discontinuities are plotting artifacts.

with what is observed experimentally. In the absence of averaging, the apparent standard deviation is overpredicted by a factor of roughly two. Various sample sizes were tested to confirm that this result was not simply an artifact of the time-averaging. Finally, the average cycle frequency (defined as one half the number of mean crossings per unit time) decreases as well due to smoothing of higher frequency signal characteristics, for instance, those corresponding to bubble coalescence.

The dynamic distribution of the solids concentration signal is particularly useful for validation purposes (7). Figure 5 clearly demonstrates that the qualitative nature of the distribution changes dramatically when a reasonable averaging scheme is implemented. There are notable differences between the single point results and the experimental data near the distributor, where void sizes tend to be smaller that the sampling volume. This tends to compress the sample variability. Also, at the higher elevation, the tail of the distribution is diminished by the averaging kernel. While the quantitative agreement with the experiment is not extremely pleasing, the properly averaged CFD data compares much more favorably. An obvious issue that could lead to discrepancies here is the validity of relating 2-D simulations to data gathered in a 3-D bed. In some earlier work (2), local time-averaged properties at mild fluidizing conditions showed fairly good agreement with experiment, despite the simulations having been performed in 2-D; at higher gas velocities, the limitations of 2-D simulations became very apparent. Therefore the present work was restricted to low superficial gas velocities.

In an actual dense fluid bed, the charge density is spatially distributed in a complex manner, with a highly charged region in the bubble wake (8). This implies the existence of a time dependent sampling volume that is influenced by the nearby charge distribution. In a more advanced simulation where conservation equations were solved for electric charge, the computed charge density could be used to compute a more accurate representation of the probe field.

SUMMARY

Rigorous validation of multiphase CFD models is best achieved on the local transient level. In contrast to integral measures (i.e., pressure), local solids concentration fluctuations are particularly attractive for accomplishing this task. During this work, needle-type capacitance probes were employed to obtain solids fluctuation time-series in a bench-scale fluidized bed. A representative two-fluid model CFD simulation was carried out. In order to draw comparisons between CFD and experiment on a one-to-one basis, a matrix of weighting coefficients was determined by numerical solution of the electric field in the vicinity of the capacitance probe. This mimics the spatial averaging intrinsic to the measurement device. While the mean solids holdup was insensitive to averaging, the standard deviation and dominant signal frequency both decreased upon application of averaging. The dynamic distribution of the properly averaged CFD signal compared qualitatively to the experimental data, while there was limited agreement in the absence of averaging. We conclude that proper characterization of the probe field is critical when utilizing data of this nature for validation of dynamic models.

NOTATION

ACF	- average cycle frequency, hz	ε_0	- permittivity of free space
E	- electric field strength, V/m	ε_S	- solids holdup
M	- # cells x-direction	μ	- index for x-dir avg
N	- # cells y-direction	ν	- index for y-dir avg
V	- voltage (potential), V	ρ	- charge density, C/m^3
W	- weighting coeff matrix		

REFERENCES

1. Grace, J.R. and F. Taghipour. *Powder Tech.*, **139** (2), 99-110 (2005).
2. Sutton, C.R. and J.C. Chen, 2005 *AIChE Annual Meeting*, Cincinatti, OH unpublished paper.
3. van Wachem, B.G.M. *et al. Chem. Eng. Sci.*, **54**, 2141-2149 (1999).
4. van Ommen, J.R. *et al. Powder Tech.*, **106**, 199-218 (1999).
5. Syamlal, M., W. Rogers, and T.J. O'Brien, *MFIX Documentation Theory Guide.* U.S. Dept. of Energy: Morgantown, WV (1993).
6. Sutton, C.R. and J.C. Chen. *I&ECR.*, **43** (18), 5776-5782 (2004).
7. Cui, H., N. Mostoufi, and J. Chaouki. *Chem. Eng. J.*, **79**, 133-143 (2000).
8. Kleijn van Willigen, F. *et al.* Fluidization XI, unpublished poster (2004).

The 12th International Conference on Fluidization - New Horizons in Fluidization Engineering, Art. 87 [2007]